DE NOVO DRUG DESIGNING FOR INFLUENZA A VIRUS H11N9, LEAD FOR NEURAMINIDASE INHIBITORS

Abstract

The study highlights the effectiveness of computer-aided *de novo* drug design, in swiftly and reliably generating novel target-specific drugs or lead-like molecules through *in silico* techniques. Using the e-Lea3D *de novo* design platform, a set of 20 distinct stereoisomers exhibiting drug/lead-like attributes were meticulously crafted within the protein's core. Emphasis was directed toward the *de novo*-generated molecules showcasing superior plant scores relative to their corresponding stereoisomers. Of 20 molecules 3 molecules were selected on the basis of high scores. Subsequent docking analyses of three selected molecules guided by the e-Lea3D outputs underscored the significance of these findings. These results hold immense promise for the advancement of potential neuraminidase inhibitors, presenting a pathway toward developing compounds with enhanced therapeutic potential.

Keywords: Neuraminidase Inhibitors, E-Lea3 D, De Novo Design, In Silico Techniques.

Authors

Archana Tomer
Department of Chemistry
Netaji Subhas University of Technology (N.S.U.T)
Erstwhile N.S.I.T, Azad Hind Fauj Marg
Dwarka, Delhi, India.
Archana.organic17@gmail.com

VishnuVats
G.B Pant DSEU Okhla-1 Campus
Delhi, India.
Vishnu.vats@dseu.ac.in

Pravita Kumar
Sri Aurobindo College Delhi
Delhi University.
dr_yogendrak@yahoo.com

Yogendra Kumar
Sri Aurobindo College Delhi
Delhi University.
Pravita.kumar@gmail.com

Anjana Sarkar
Department of Chemistry
Netaji Subhas University of Technology (N.S.U.T)
Erstwhile N.S.I.T, Azad Hind Fauj Marg
Dwarka, Delhi, India.
anjisarkar@gmail.com

I. INTRODUCTION

Influenza viruses classified inside the family *Orthomyxoviridae* exhibit genetic diversity due to mutations or gene re-assortments, leading to drift or shift (1)(2). Seasonal outbreaks of acute respiratory diseases are mostly due to Influenza A and B viruses resulting in a significant annual death toll ranging from 290,000 to 650,000 people. Over the past 150 years, there have been a minimum of five instances of influenza A virus pandemics including the Spanish flu (1918–1920), Asian flu (1957–1958), Hong Kong flu (1968–1969), Russian flu (1977–1979), and Swine flu (2009–2010) causing a loss of millions of lives worldwide. (3). As of January 2021 data from FLUnet, the majority of tests carried out by WHO, the tested specimens were positive for type B influenza viruses instead of type A influenza, under the framework of the Global Influenza Surveillance and Response System (GISRS). There exist 11 neuraminidase (NA) variants and 18 hemagglutinin (HA) variants within these viruses (3). Several of these variants like (H1–H3, H5–H7, H9, N1–N2, and N6–N9) have been identified in diverse hosts, including poultry, swine, and humans. Neuraminidase plays a crucial role in modern anti-influenza drug discovery efforts, as it is a significant target and serves as a key enzyme in the life stages of the influenza virus, aiding in viral release and transmission. Neuraminidase (NA) primarily functions to aid in the elimination of sialic acid bound to glycoprotein receptors present on cell surfaces. This action plays a crucial role in enabling the virus to disseminate and initiate infection in new cells.(4).

Neuraminidase is among the surface glycoproteins found in influenza-type family. Its primary role involves severing terminal sialic acid from cell surfaces linked to glycol-conjugated surfaces, which act as receptors for hemagglutinin. Blockage of NA slows the discharge of new viral particles, reducing viral transmission and allowing the immune system to eliminate the viruses effectively. NA is composed of four identical monomers, forming a tetramer. On the basis of sequence analysis, two distinct phylogenetic groups encompass Neuraminidases (NAs). Group 1 neuraminidases (N1, N4, N5, and N8) exhibit an open conformation 150-loop active site, while group 2 neuraminidases (N2, N3, N6, N7, and N9) have a closed conformation 150-loop active site(5).The CDC endorses four FDA-approved drugs for treating influenza viruses: Oseltamivir, Zanamivir, Peramivir, and Baloxavir marboxil. The effects of the H11N9 strain on avian and humans are currently unknown. However, it is worth mentioning that the H7N9 strain which caused severe illness and deaths in humans is suspected to have originated from either the H11N9 or H2N9 strains, specifically regarding the NA component(6).Neuraminidase inhibitors are commonly used as antiviral medications to treat patients with increased susceptibility to influenza-related complications. The well-known neuraminidase inhibitors include, Zanamivir, Oseltamivir, Peramivir, and Laninamivir(7) (8)(9)(10),These drugs have been effective in combating influenza; however, there have been reports of emerging resistance highlighting the requirement for improved treatment options Baloxavir marboxil, a cap-binding endonuclease blocker is a recently approved drug that offers an alternative treatment option(11). Laninamivir is currently approved only in Japan(12)(13). The integration of computational methodologies, such as *de novo* design opens doors for accelerating drug discovery and design processes, ultimately contributing to the field of drug development and targeted treatment strategies.

II. MATERIAL AND METHODOLOGY

1. **3D Structure of a Target:** Researchers explored the Protein Data Bank (PDB) database in search of the 3D crystal structure of N9 neuraminidase originating from Influenza and type A.(strain A/Tern/Australia/G70C/1975(H11N9)). The search criteria included the X-ray crystallography method, the best resolution and the best global validation metrics for protein retrieval. Among the available X-ray crystallography structures, the one with PDB ID: 6HCX at a resolution of 1.30 Å and the best global validation metrics, was selected for further analysis. This structure represented a monomer with chain A and was complexed with Zanamivir. Chain A consisted of 388 amino acids (AA) spanning from ARG83 to LEU470. Other neuraminidase structures were not considered due to poor resolution, mutant protein structure, artificial re-assortment, missing residues, or lower global validation metrics, as per the PDB X-ray structure validation criteria(14).

2. **Active site:** In all NA subtypes, there are pivotal role of amino acid components situated within the active site in enabling the catalytic function of the NA enzyme. These amino acid components include ARG118, ARG152,ARG224 ARG292, ARG371, ASP151, GLU276, and TYR406.The active site's three-dimensional structure comprises ARG156, ASP198,ASP293, GLU227, GLU425, GLU119, ILE222, , SER179, , and TRP178 .Interactions between the target 6HCX and the ligand Zanamivir at the active site including both hydrogen and non-hydrogen bond interactions were examined using LIGPLOT. The LIGPLOT interactions, which represent the active pocket of the target 6HCX with Zanamivir, were obtained from PDBsum (**Figure1b**)

3. **Protein Preparation:** For the preparation of protein for docking, specific components of the PDB structure 6HCX, including heteroatoms, water molecules, and ligand groups, were cleaned using Discovery Studio Visualizer **(Figure1a and 1b).**
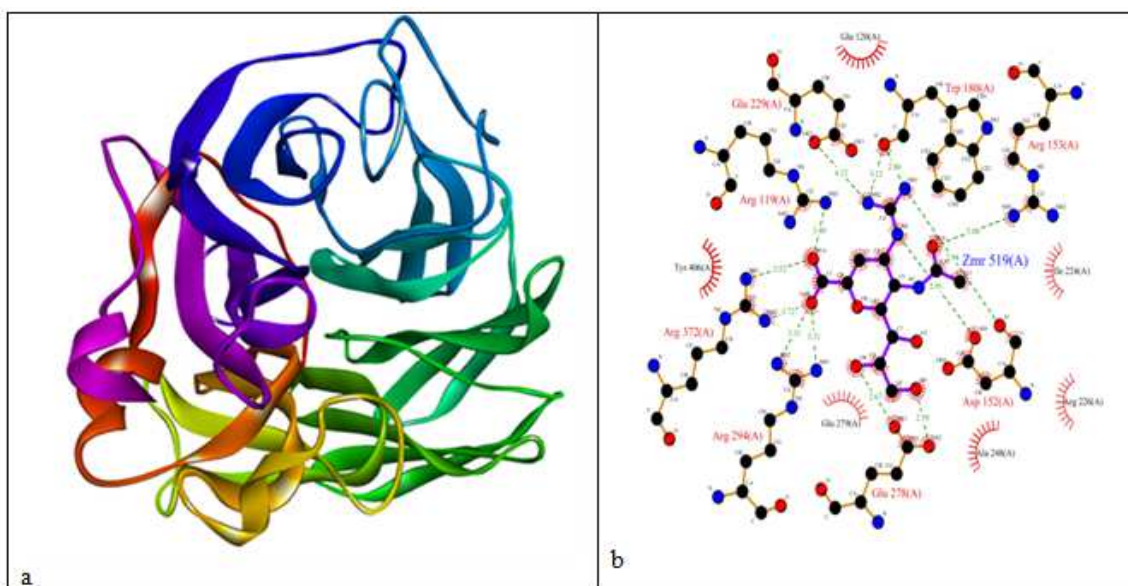

Figure 1(A-B) : 3D Structure of 6HCX Chain A, B LIGPLOT of Interactions Involving Ligand Zanamivir with 6HCX Amino Acid Residues

4. **ADME Prediction:** The assessment of ADME properties was conducted using the Swiss ADME web server (absorption, distribution, metabolism, and excretion). This system is used to predict various physicochemical attributes, such as lipophilicity, water solubility, pharmacokinetics, and adherence to key drug-likeness rules (like Lipinski, Ghose, Veber, Egan, Mugge, and Bioavailability score). Among these, the widely cited Lipinski rule offers valuable insights into a ligand's potential as a drug candidate, stipulating the below criteria:

Molecular weight under 500.

Octanol-water coefficient (logP) less than 5.

Up to 5 hydrogen bond donors and no more than 10 hydrogen bond acceptors are allowed.

Built upon Lipinski's rule, compounds have progressed to the stage of pre-filtration for identifying promising drug candidates. This preliminary filtering of drug candidates serves to secure their pharmacological relevance and potential

This was employed for the prediction of drug-likeness and potential interactions of the drugs with cytochrome P450 enzymes (15)(16).

5. **De Novo Designing using E-LEA3D:** The e-LEA3D web server was utilized to conduct computer-aided de novo drug design. This tool generates fresh compounds either by starting from square one or using a tailored scaffold featuring optimized substituents as defined by the user. The approach is fragment-based, utilizing a genetic algorithm for the enhancement of fragment combinations. The protein structure was uploaded onto the e-LEA3D web server, and the binding site coordinates were adjusted to match the predicted activity (X= 17.89466812, Y = 20.99328986, Z= 55.71566522). The parameters for the radius binding site (10A) and weight in the final score (1) were personalized. However, the genetic algorithm parameters, like the number of generations, population size, and other molecular properties, were adjusted to their default values(17).The visualization of the acquired results was carried out using Discovery Studio software.

III. RESULT & DISCUSSION

1. **ADME Properties:** De novo drug design is an automated computational process that constructs molecules targeting specific biological targets using atoms or fragments. The goal is to create molecular structures that meet the criteria for in silico drug/lead likeness. In our study, we successfully designed novel molecules within the active pockets using the de novo technique with a updated edition of the LEA3D webserver. From the e-LEA3D output, we obtained 20 molecules, but only three were taken into account. **(Table 1 and Figure 2(a-c))** The others were excluded based on score and constraint applied during in ADMET screening and silico drug/lead likeness which included the evaluation of Lipinski's rule of 5. In line with the rule, for a molecule to be a potential oral drug, it should not violate multiple of the defined rule's .
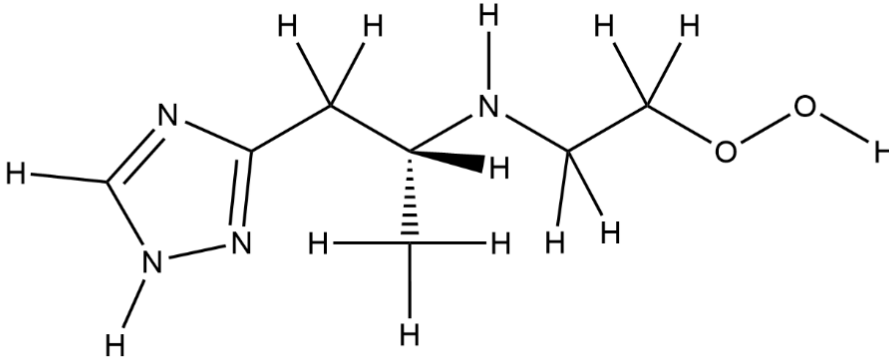
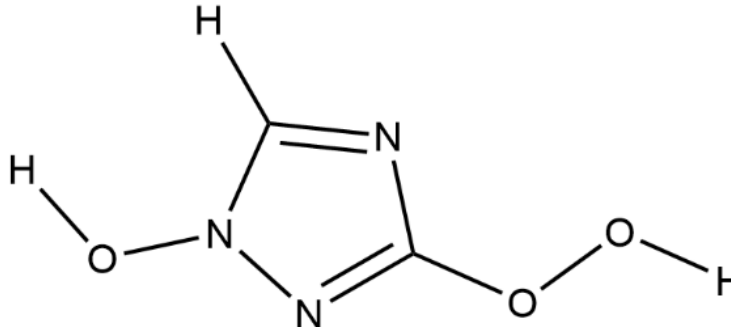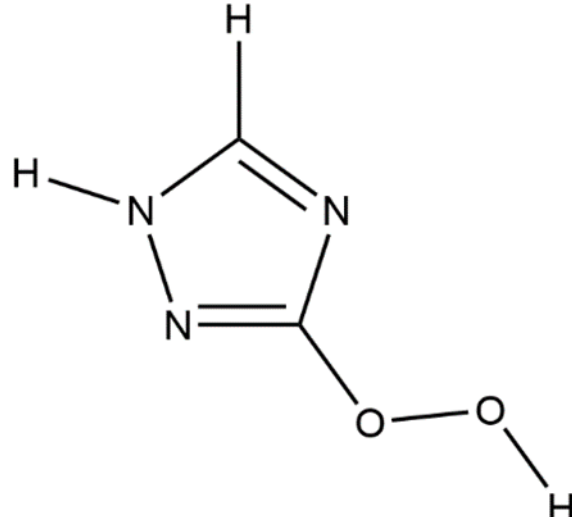| 14 | 1 | Click to display

(or download the sdf file)

Complex with proteinh.pdb:

Click to display

see the docking log file

(download site_and_ligand.pdb)

(download fullcomplex.pdb)

(download docked_conformation.mol2) | 42.32 | Conformer
PLANTS_score_chemplp
proteinh.pdb()

1 -63.480 -63.480 | 1*1-2*3_1*17-3*1

921 138 1207 | 1 conformers

Best is no 1 |

a

| 20 | 1 | Click to display

(or download the sdf file)

Complex with proteinh.pdb:

Click to display

see the docking log file

(download site_and_ligand.pdb)

(download fullcomplex.pdb)

(download docked_conformation.mol2) | 38.61 | Conformer
PLANTS_score_chemplp
proteinh.pdb()

1 -57.910 -57.910 | 1*3-2*1_2*1-3*1_1*5-4*1

138 946 1207 1207 | 1 conformers

Best is no 1 |

b

| 15 | 1 | Click to display

(or download the sdf file)

Complex with proteinh.pdb:

Click to display

see the docking log file

(download site_and_ligand.pdb)

(download fullcomplex.pdb)

(download docked_conformation.mol2) | 35.65 | Conformer
PLANTS_score_chemplp
proteinh.pdb()

1 -53.470 -53.470 | 1*1-2*3_1*1-3*1

946 138 1207 | 1 conformers

Best is no 1 |

c

Figure 2 :(a-c)) De Novo Drug Design Top Score Results

Table1: Generated Compounds

S.no	Potential Ligands
1	 (*R*)-*N*-(2-hydroperoxyethyl)-1-(1*H*-1,2,4-triazol-3-yl)propan-2-amine
2	 3-hydroperoxy-1*H*-1,2,4-triazol-1-ol
3	 3-hydroperoxy-1*H*-1,2,4-triazole

The initial screening process for potential life-saving drug candidates involved the application of Lipinski's Rule of 5. This rule examines key parameters like Hydrogen Bond Donor (HBD) count, Molecular Weight (M.Wt), Hydrogen Bond Acceptor (HBA) count, Octanol-Water Partition Coefficient (logP), and molar refractivity index. The evaluation of all three compounds against these criteria are mentioned in **Table2.** These Schiff bases not only met the stringent criteria of the first assessment but also conformed to Veber's law which gauges the bioavailability score of drug candidates. The calculated bioavailability score for these was 0.55. Furthermore, the Synthetic Accessibility (SA) of the compound was determined to be within the favorable range of greater than 1 and less than 10 which signifies the ease of synthesizing these compounds in a laboratory setting. The consideration of Synthetic Accessibility is pivotal in the selection process of drug design and its integration into computer-aided design (CAD) workflows can significantly enhance the efficiency and success rates of drug development endeavors. In essence, these findings collectively underscore the promising potential of these designed compounds as viable candidates for further drug design and development.

Table2: Druglikeness Parameters of Compounds

| Drug Likeness Property Parameter	Compounds		
	1	**2**	**3**
M.Wt <500	186	117	101
HBA <5	3	5	4
HBD<10	5	2	2
logP <5	1.10	0.54	0.06
Lipinski Rule	Yes	Yes	Yes
Bioavailability score	0.55	0.55	0.55
Veber's Rule	Yes	Yes	Yes
Synthetic accessibility	3.04	3.05	2.56

2. **Molecular Docking Analysis:** In the process of de novo drug design, an assessment was conducted on a total of 420 molecules. Subsequently, the software generated results for the top 20 molecules. From this subset, focused attention was directed toward the investigation of the top 3 molecules, which were to be selected on the basis of their highest scores. Compound 1 exhibited the most elevated score of 42.32, while compound 2 achieved a score of 38.61, and compound 3 obtained a score of 35.65. These results establish their superior performance compared to the other compounds within the designed molecule set. Among all the designed molecules, compounds 1, 2, and 3 maintained their leading positions. This high score is a positive indicator of the strong connection between the target protein and compound. The docking results obtained from e-LEA3D output of compounds (1-3) with the target protein 6HCX are summarized in Table3. The 2D and 3D structures of the docked compound (1-3) are illustrated in Figure 3(a-c) and Figure 4 (a-c) respectively. It is of significant importance that compound 1 exhibited interaction involving 5 hydrogen bonds, compound 2 displayed 6 hydrogen bonds, and compound 3 demonstrated 4 hydrogen bonds. These observations underline the substantial affinity between these compounds and the protein complex. The

comprehensive details provided in Table 3 shed light on the distinct binding characteristics of these three compounds and their potential as promising candidates for further exploration in protein-ligand interactions.

Table 3: 2D Interaction of 6HCX and Compounds (1-3)

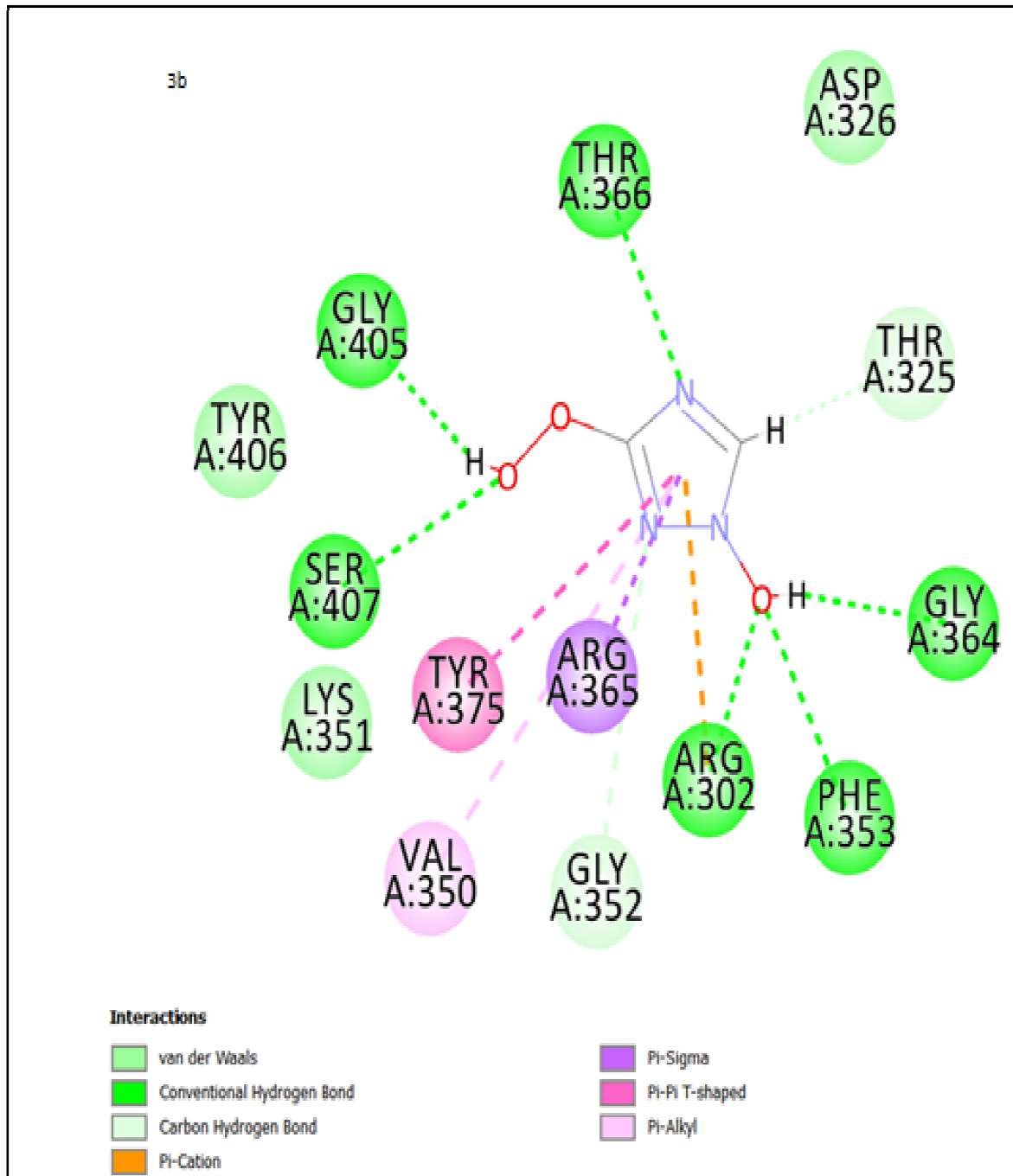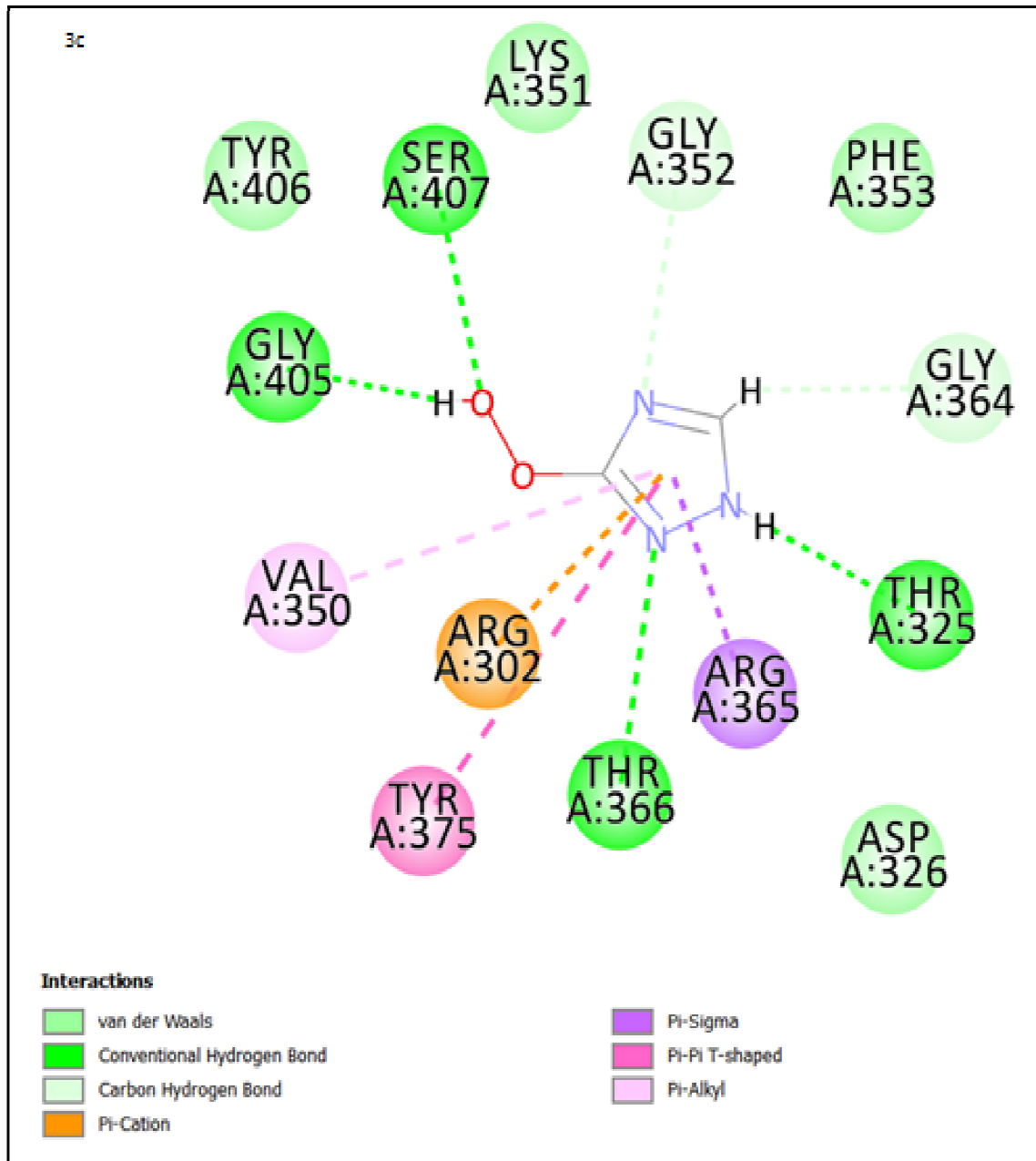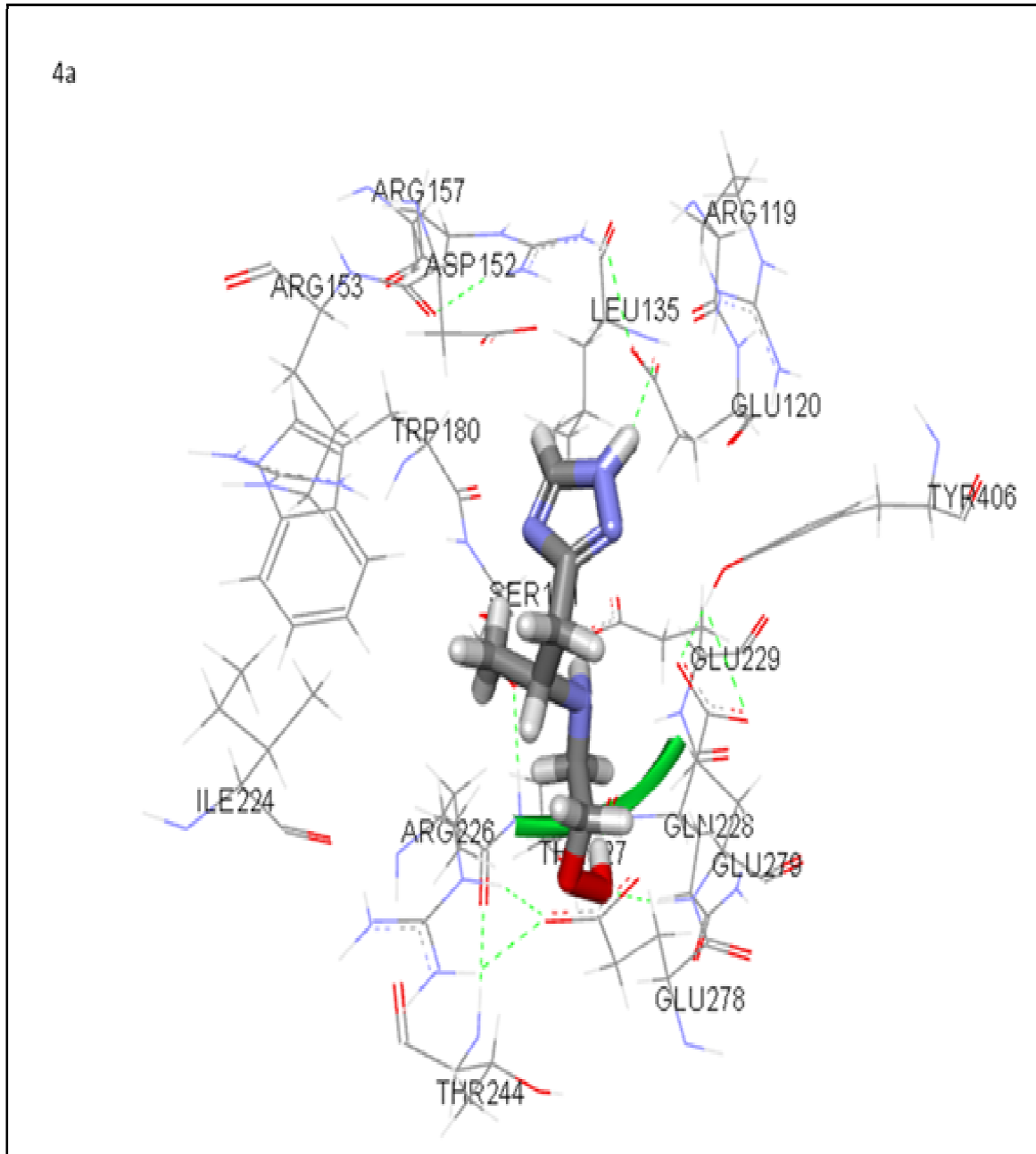| Target Protein (Pdb Id)	Generated Compound	Interacting Amino Acid at the Active Site	Interaction Type	H-Bond	Score
6HCX	**1**	GLU120,ASP152,THR227,GLU229,GLU279,TYR406	H-bond Van der Waals Pi-anion	5	42.32
	2	THR325,ARG302, VAL350, ARG365,THR366, TYR375,GLY405,SER407, PHE253	H-bond Van der Waals Pi-alkyl Pi-Cation Pi-Sigma Pi- Pi T-shaped	6	38.61
	3	ARG302,THR325, VAL350, ARG365,THR366, TYR375 GLY405,SER407	H-bond Van der Waals Pi-alkyl Pi-Cation Pi-Sigma Pi- Pi T-shaped	4	35.65
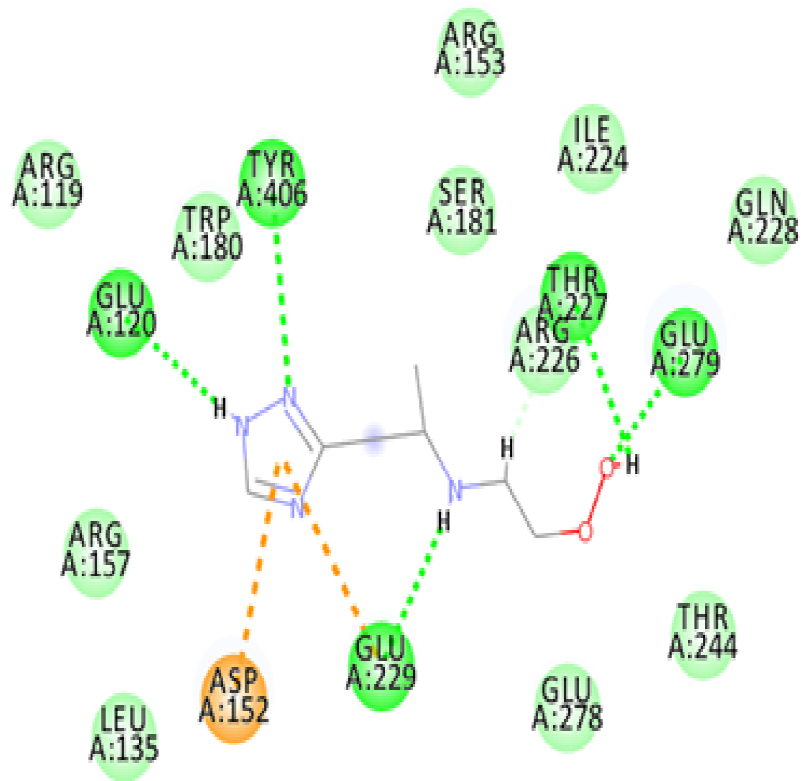
Figure 3 :(a-c) 2D Interaction between Targeted Proteins, PDB ID: 3T88 with Generated Compounds (1-3 Respectively
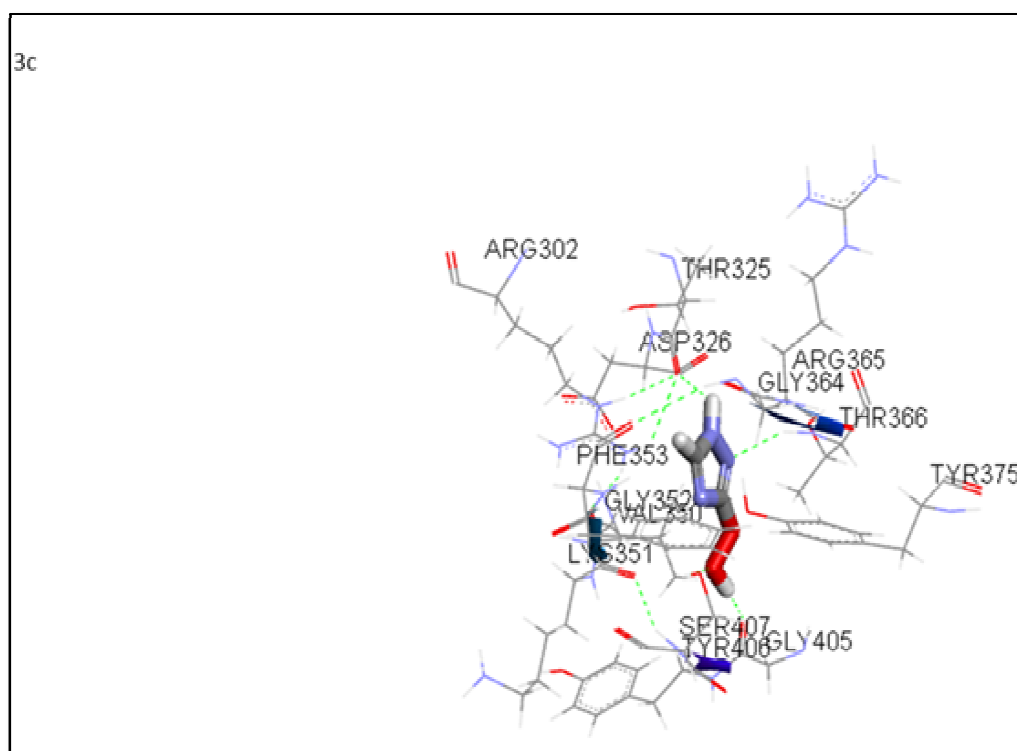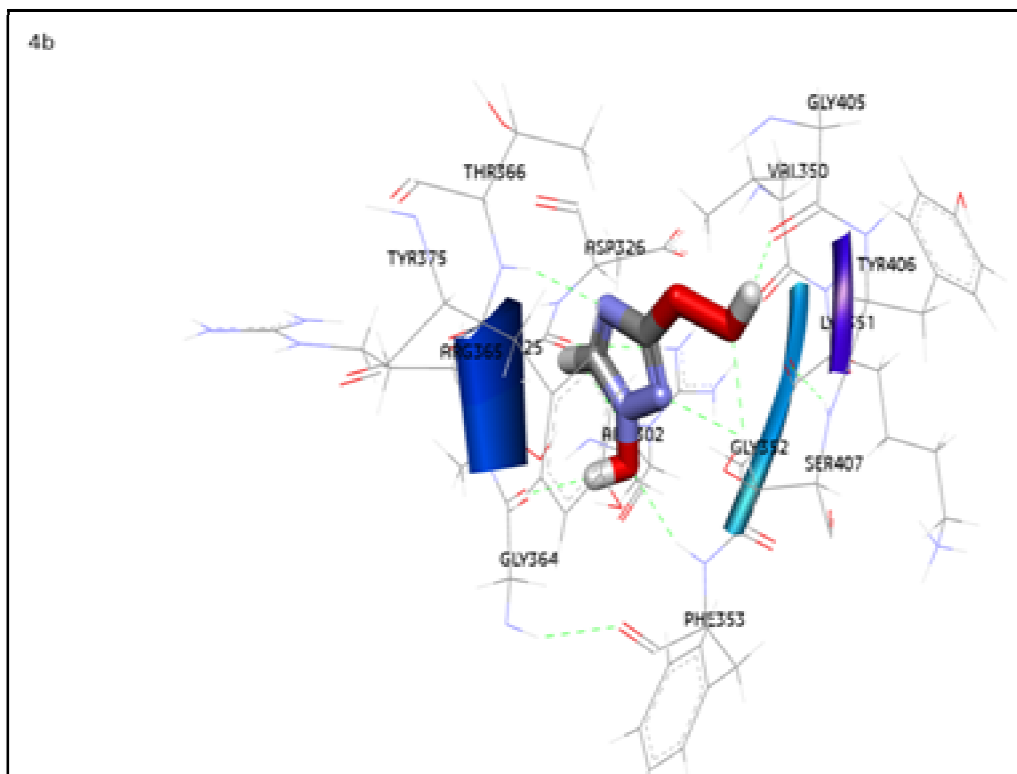
Figure 4 :(a-c) 3D Interaction between Targeted Proteins PDB ID: 3T88 with Generated Compounds (1-3 Respectively)

IV. CONCLUSION

Computer-aided *de novo* drug design represents a rapid and dependable *in silico* approach for creating new target-specific drugs or molecules with lead-like properties. In this probe, the e-Lea3D *de novo* design platform has been employed to scrutinize 20 distinct stereoisomers with drug/lead-like properties within the protein's core. The focus was placed on the *de novo*-generated molecules that displayed the highest plant scores among their respective stereoisomers. Three molecules having the highest scores were subsequently subjected to docking analyses, utilizing the outcomes provided by the e-Lea3D website. These compounds possess the potential to contribute significantly to the advancement of promising neuraminidase inhibitors.

REFERENCES

[1]   Ziegler T, Mamahit A, Cox NJ. 65 years of influenza surveillance by a World Health Organization-coordinated global network. Influenza Other Respi Viruses. 2018;12(5):558–65.

[2]   Hofer U. Viral evolution: Past, present and future of influenza viruses. Nat Rev Microbiol. 2014;12(4):237.

[3]   Adlhoch C, Delgado-Sanz C, Carnahan AS, Larrauri A, Popovici O, Bossuyt N, et al. Effect of neuraminidase inhibitor (oseltamivir) treatment on outcome of hospitalised influenza patients, surveillance data from 11 EU countries, 2010 to 2020. Euro Surveill [Internet]. 2023;28(4). Available from: http://dx.doi.org/10.2807/1560-7917.ES.2023.28.4.2200340

[4]   Smith BJ. Analysis of inhibitor binding in influenza virus neuraminidase. Protein Sci. 2001;10(4):689–96.

[5]   Li Q, Qi J, Zhang W, Vavricka CJ, Shi Y, Wei J, et al. The 2009 pandemic H1N1 neuraminidase N1 lacks the 150-cavity in its active site. Nat Struct Mol Biol [Internet]. 2010;17(10):1266–8. Available from: http://dx.doi.org/10.1038/nsmb.1909

[6]   Tuong HT, Nguyen NM, Sung HW, Park H, Yeo SJ. Genetic characterization of avian influenza A (H11N9) virus isolated from Mandarin ducks in South Korea in 2018. Viruses. 2020;12(2).

[7]   Jefferson T, Jones M, Doshi P, Spencer EA, Onakpoya I, Heneghan CJ. Oseltamivir for influenza in adults and children: Systematic review of clinical study reports and summary of regulatory comments. BMJ. 2014;348(April):1–18.

[8]   Heneghan CJ, Onakpoya I, Thompson M, Spencer EA, Jones M, Jefferson T. Zanamivir for influenza in adults and children: Systematic review of clinical study reports and summary of regulatory comments. BMJ. 2014;348(April):1–16.

[9]   Ishizuka H, Yoshiba S, Okabe H, Yoshihara K. Clinical pharmacokinetics of laninamivir, a novel long-acting neuraminidase inhibitor, after single and multiple inhaled doses of its prodrug, CS-8958, in healthy male volunteers. J Clin Pharmacol. 2010;50(11):1319–29.

[10]   Mclaughlin MM, Skoglund EW, Ison MG. Peramivir: An intravenous neuraminidase inhibitor. Expert Opin Pharmacother. 2015;16(12):1889–900.

[11]   Kumar D, Ison MG, Mira J-P, Welte T, Hwan Ha J, Hui DS, et al. Combining baloxavir marboxil with standard-of-care neuraminidase inhibitor in patients hospitalised with severe influenza (FLAGSTONE): a randomised, parallel-group, double-blind, placebo-controlled, superiority trial. Lancet Infect Dis [Internet]. 2022 May 1;22(5):718–30. Available from: https://doi.org/10.1016/S1473-3099(21)00469-2

[12]   Sunagawa S, Higa F, Cash HL, Tateyama M, Uno T, Fujita J. Single-dose inhaled laninamivir: Registered in Japan and its potential role in control of influenza epidemics. Influenza Other Respi Viruses. 2013;7(1):1–3.

[13]   Lackenby A, Besselaar TG, Daniels RS, Fry A, Gregory V, Gubareva L V., et al. Global update on the susceptibility of human influenza viruses to neuraminidase inhibitors and status of novel antivirals, 2016–2017. Antiviral Res [Internet]. 2018;157:38–46. Available from: https://doi.org/10.1016/j.antiviral.2018.07.001

[14]   Burley SK, Berman HM, Bhikadiya C, Bi C, Chen L, Di Costanzo L, et al. Protein Data Bank: The single global archive for 3D macromolecular structure data. Nucleic Acids Res. 2019;47(D1):D520–8.

[15]   Daina A, Michielin O, Zoete V. SwissADME: A free web tool to evaluate pharmacokinetics, drug-likeness and medicinal chemistry friendliness of small molecules. Sci Rep. 2017;7(January):1–13.

[16] Kesh M, Goel S. Target-Based Screening for Lead Discovery. 2023. 141–173 p.

[17] Douguet D. e-LEA3D: a computational-aided drug design web server. Nucleic Acids Res [Internet]. 2010 Jul 1;38(suppl_2):W615–21. Available from: https://doi.org/10.1093/nar/gkq322